Mechanics & Industry **19**, 109 (2018)
© AFM, EDP Sciences 2018
https://doi.org/10.1051/meca/2018018

Mechanics & Industry

Available online at:
www.mechanics-industry.org

Regular Article

An adaptive LQR controller based on PSO and maximum predominant frequency approach for semi-active control scheme using MR Damper

Gaurav Kumar*, Ashok Kumar, and Ravi S. Jakka

Department of Earthquake Engineering, Indian Institute of Technology, 247667 Roorkee, Uttarakhand, India

Received: 12 July 2017 / Accepted: 4 March 2018

Abstract. In the linear quadratic regulator (LQR) problem, the generation of control force depends on the components of the control weighting matrix **R.** The value of **R** is determined while designing the controller and remains the same later. Amid a seismic event, the responses of the structure may change depending the quasi-resonance occuring between the structure and the earthquake signal. In this situation, it is essential to update the value of **R** for conventional LQR controller to get optimum control force to mitigate the vibrations due to the earthquake. Further, the constant value of the weighting matrix **R** leads to the wastage of the resources using larger force unnecessarily where the structural responses are smaller. Therefore, in the quest of utilizing the resources wisely and to determine the optimized value of the control weighting matrix **R** for LQR controller in real time, a maximum predominant period $\tau_p^{\max}$ and particle swarm optimization-based method is presented here. This method comprises of four different algorithms: particle swarm optimization (PSO), maximum predominant period approach $\tau_p^{\max}$ to find the dominant frequency for each window, clipped control algorithm (CO) and LQR controller. The modified Bouc-Wen phenomenological model is taken to recognize the nonlinearities in the MR damper. The assessment of the advised method is done on a three-story structure having a MR damper at ground floor subjected to three different near fault historical earthquake time histories. The outcomes are equated with those of simple conventional LQR. The results establish that the advised methodology is more effective than conventional LQR controllers in reducing inter-story drift, relative displacement, and acceleration response.

Keywords: Maximum predominant period / PSO / LQR / MR damper

1 Introduction

The increasing need for measures against the vibration, use of vibration dampers, and avoidance technologies became a lucrative field for researchers and engineers worldwide. They are working rigorously to make infrastructures safer for the humans through various means. Structural vibration control has proved very helpful for this purpose. Generally, large intensity earthquakes may lead to more perilous forces on the higher floors. For the safety of the structure and its occupants, it is necessary to increase the resistance of the normal structure against earthquake by incorporating control mechanism. In 1972, Yao gave the notion of structural control since then this field has emerged by leaps and bounds [1].The vibrations in the structure can be kept in control by altering its stiffness, providing extra damping and applying appropriate passive, active or semi-active counterforce, however, its dynamic properties ought to remain unaltered [2]. To date, a few control strategies like active passive and semi-active were employed commendably which offer the prospects of developing applications, improving efficacy and provide better acceptability. Out of these, the semi-active control strategy is being considered as a promising choice for structural control nowadays. Semi-active control scheme generally uses the dampers which have rheological properties e.g. magneto-rheological (MR) damper [3]. The rheological materials used in MR dampers are capable of varying their physical appearance proactively using very low power [4]. The MR dampers can only absorb energy which is being produced due to vibrations in the structure by responding to its motion. Therefore, bounded input bounded output (BIBO) stability is assured [5]. A model to exhibit the capacities of the MR damper in light of the Bouc-Wen hysteresis hypothesis was introduced in 1997 and employed successfully in a number of studies on semi-active control strategy [4,6,7]. Several experiments were

* e-mail: sainideq@iitr.ac.in

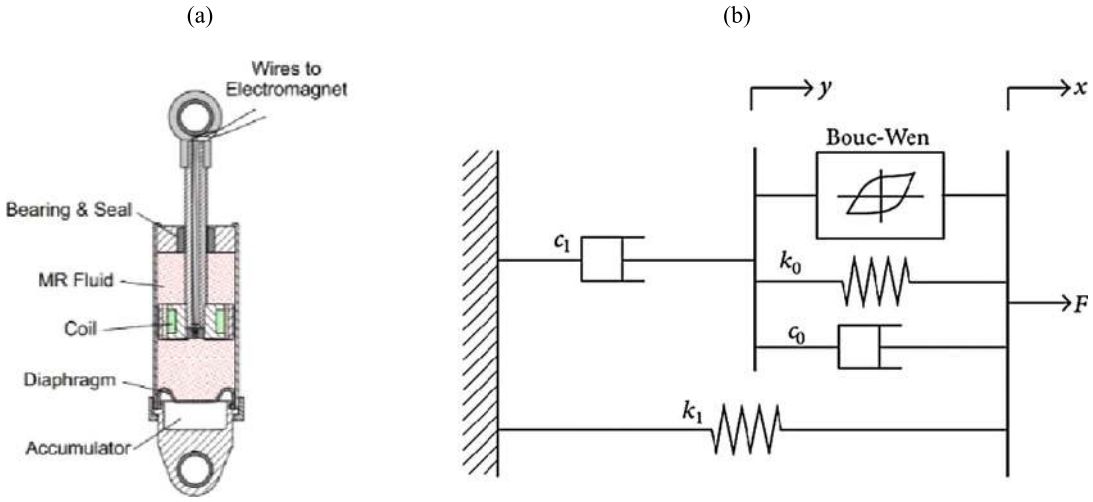

Fig. 1. (a) The cross-section of the MR damper (b) The modified mechanical Bouc-Wen model [6].

conducted on a scaled three-story prototype structure having a MR damper which established the fact that the effectiveness of a controller very much relies on the algorithm used [8–11]. Some very commonly controllers are LQR controller, sliding mode controller, LQG/H_2 controller, fuzzy logic controller etc. [7,12–19].

Here in this approach, the LQR controller is considered due to its simplicity though it has some inherent issues reported in the literature [6], [20,21]. Panariell et al. (1997) [22] proposed an algorithm based on carrying up-to-date weighting matrices for the gain of the LQR controller from a database of documented earthquake excitations. The need for an offline repository of known earthquakes was the limitation in this study. Keeping this limitation in mind, Basu et al. (2008) [23] introduced modified TVLQR method by updating weighting matrices using a constant multiplier on the basis of DWT analysis. The value of this constant multiplier is decided by the energy content in the distinctive frequency groups over a period window and lies in the range of [0,1]. Although the weighting matrices vary at resonance condition, the constant multiplier was chosen offline in this method. Therefore, offline data were still a requirement [23,24]. The effectiveness of the LQR controlled system depends on many parameters e.g., the state weighting matrix **Q** and the control weighting matrix **R**. Although, difficult but the selection of these matrices is preceded by a lot of experimentation during designing of the controller. Because these parameters directly influence the effectiveness of the LQR controller, to determine them correctly in real time is essential for their application in structural control.

In this article, a modified LQR method is presented to determine the optimized value of control weighting matrix **R** for tracking down the optimal control force of MR damper in real time using PSO and maximum dominant period $\tau_p^{\max}$. Every optimized control weighting matrix is governed by a small group of frequency, therefore, vulnerabilities in system parameters can't influence them. The controller thus obtained has low-frequency switching prerequisites unlike conventional LQR because the updating of the gain occurs only after an interval of a time window. The advantage of using maximum dominant period $\tau_p^{\max}$ makes the proposed controller inherently fast in comparison to the controllers which employ time-frequency approaches like WVT, STFT, DWT etc. [24,25]. A three-story structure integrated with a MR damper at ground floor is chosen to validate the efficacy of the suggested approach. The results are equated with those obtained using conventional LQR controller. It establishes the ability of the proposed method in reducing the vibrations during the event of an earthquake. Moreover, the modified LQR controller not only decreases the relative displacement, inter-storey drift and acceleration responses of structures considerably but also reduces the cumulative energy demand.

2 Modeling of magnetorheological damper

MR damper force relies on the displacement of the structure and is highly nonlinear in nature. Therefore, a model is required to realize the nonlinearities in the MR damper. In light of the Bouc-Wen hysteresis model (Wen, 1976) a phenomenological model was given by Spencer et al. (1997) [4]. This model was henceforth used to demonstrate the capacities of MR dampers [5–9].

Equations (1)–(7) represent this model shown in Figure 1(b).

$$F = c_1\dot{y} + k_1(x_1 - x_0), \tag{1}$$

$$\dot{y} = \frac{1}{(c_0 + c_1)}\{\alpha z + c_0\dot{x}_1 + k_0(x_1 - y)\}, \tag{2}$$

$$\dot{z} = -\gamma|\dot{x}_1 - \dot{y}||z|^{n-1} - \beta(\dot{x}_1 - \dot{y})|z|^n + A(\dot{x}_1 - \dot{y}), \tag{3}$$

$$\alpha = \alpha_a + \alpha_a u, \tag{4}$$

$$c_1 = c_{1a} + c_{1b}u, \tag{5}$$

$$c_0 = c_{0a} + c_{0b}u, \tag{6}$$

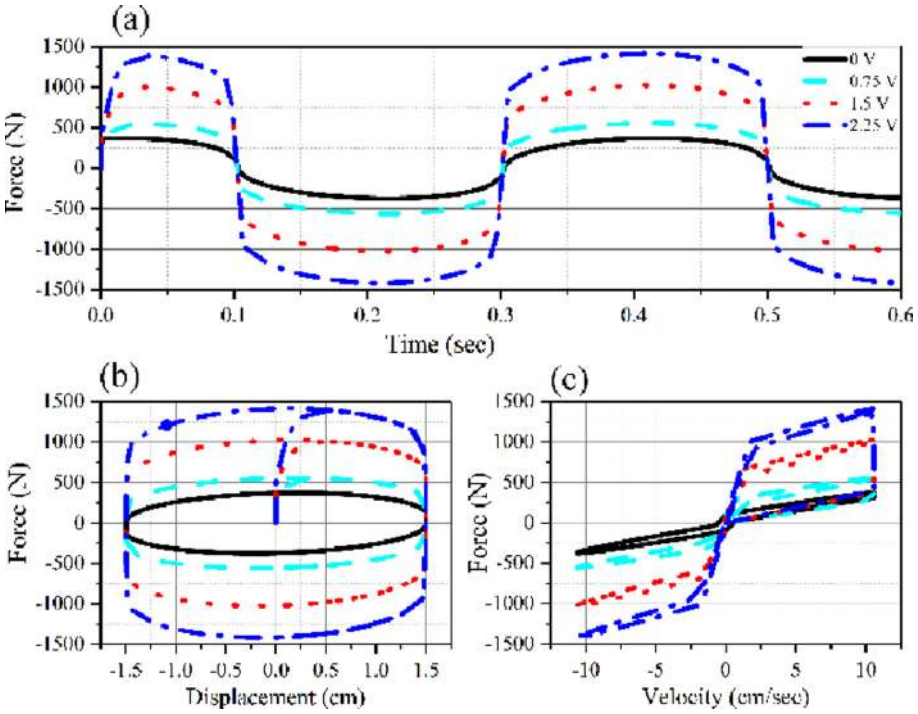

Fig. 2. MR damper response to a 2.5 Hz sinusoidal excitation with an amplitude of 1.5 cm (a) Simulated force history (b)Force-displacement (c) Force −Velocity.

$$\dot{u} = -\eta(u - v). \tag{7}$$

The variable k_1 shows the stiffness of the accumulator and a very small accumulator force is represented by its initial displacement x_0. The dashpots c_0 and c_1 represent the damping perceived at large and low velocities respectively. The parameter k_0 represents the stiffness at large velocities. The variables α, β, γ and A are the hysteresis parameters for the MR liquid. An evolutionary parameter z expresses the mechanism of reliance of the response on history. A first order filter is given in equation (7) with its output effective voltage u and commanded voltage v. This first order filter demonstrates the dynamics involved in attaining the rheological equilibrium by the MR damper [4,25]. The parameters of the commercial MR damper are given in Dyke et al. [9] utilized as a part of the present work. Simulation tests were conducted on the damper applying different voltage levels to characterize its mechanical attributes as shown in Figure 2a–c

3 The proposed approach

3.1 The PSO algorithm

The PSO algorithm was discovered in the 1990s by Kennedy and Eberhart. The PSO algorithm [26] begins with an arbitrary populace (swarm) of people (particles) in the hunt space and chips away at the social conduct of the particles in the swarm. The position and the velocity of the kth particle in the d-dimensional pursuit space can be symbolized as in equations (8)–(9).

$$Q_k = \left[q_{(k,1)}, q_{(k,2)}, q_{(k,3)}, q_{(k,4)}, \ldots\ldots q_{(k,d)}\right], \tag{8}$$

$$\dot{Q}_k = \left[\dot{q}_{(k,1)}, \dot{q}_{(k,2)}, \dot{q}_{(k,3)}, \dot{q}_{(k,3)}, \dot{q}_{(k,d)},\right], \tag{9}$$

where Q and $\dot{Q}$ represent the position and velocity of the particles. Every particle must have its own best position related to individual best objective value attained by now at time t as in equation (14). The global best particle (G_{best}) characterizes the best particle found by this time in the entire swarm at the same time t [19,27]. The updated velocity of each particle is given as in equation (10).

$$\dot{q}_{k,j}(t+1) = \partial \dot{q}_{k,j}(t) + a_1 b_1 + a_2 b_2 \left(G_{\text{best}}(t) - q_{k,j}(t)\right). \tag{10}$$

Here, j is a real positive integer and can have value $j = 1,2.....d$, where d is a natural number. Here, a_1 and a_2 are acceleration coefficients ∂ is the inertia factor and b_1 and b_2 are two independent arbitrary numbers unvaryingly dispersed in the range of [0,1]. The position update of each particle in each generation is given in equation (11).

$$q_{k,j}(t+1) = q_{k,j}(t) + \dot{q}_{k,j}(t+1). \tag{11}$$

The objective function for the PSO algorithm for each ground motion is dependent on the displacement of the structure and is represented as in equation (12) in terms of

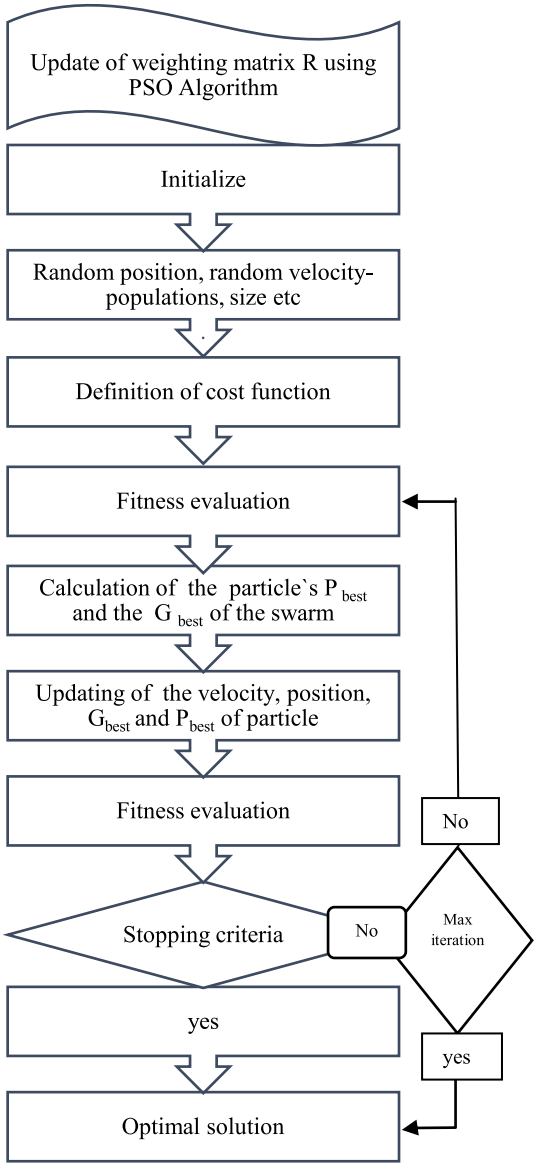

Fig. 3. Flowchart representation of PSO algorithm.

the displacement $x_k(t)$ of the kth floor

$$J_{\mathrm{PSO}} = \int_0^{t_i} \{x_{k+1}(t) - x_k(t)\}^2 dt. \tag{12}$$

The control weighting matrix **R** decreases when the structure has higher displacement due to the earthquake. This lessening of weighting matrix **R** sets off the reduction of structural response without any loss. Therefore, the merit of the advised modified LQR method is that the gain matrices are ascertained adaptively by PSO algorithm, unlike time-varying LQR case described by Basu et al. [23]. In PSO algorithm, the solution obtained via meeting the stopping criteria is considered the optimal solution. If the algorithm is going to execute maximum iteration, it may not be the optimal solution. Going for the maximum iteration means that the algorithm did not find the best optimal solution yet. To find the optimal solution now we need to vary the parameter of the PSO algorithm and run the simulation again in the quest for optimal solution via stopping criteria. The flowchart of PSO algorithm is given in Figure 3.

The maximum predominant period based modified LQR controller formulation

Earthquakes are a highly non-stationary signal having many frequency components. The frequencies in the earthquake excitation near to the natural frequency of the structure cause quasi-resonance which further leads to the higher structural response that requires higher control force for effective structural control. Usually, in a LQR problem, the control effort depends on the components of the weighting matrix R. In the conventional LQR algorithm, the state weighting matrix **Q** and control weighting matrix **R** usually are determined only while designing the controller. These matrices have global values and are not updated when quasi-resonance causes high structural response. Therefore, to mitigate the effect of quasi-resonance, the conventional LQR must be amended by determining the optimized weighting matrices in real time. This will also enhance the performance of the controller by saving the energy for non-resonant bands (i.e. where quasi-resonance does not occur). The acceleration response of the structure reflects properties like earthquake excitation. So, entire duration of this response (0, t) is divided further into smaller time windows, with the ith window being (t_{i-2} t_i). Maximum predominant period $\tau_p^{\max}$ is used to find the dominant frequency for each time window. This keeps the system always in the time domain and thus the controller becomes inherently fast. Originally, the idea of the maximum predominant period τ_p was first introduced by Nakamura [28], to classify large and small earthquake based on frequency content present in the earthquake signal. The parameter $\tau_{p,i}$ can be calculated from the acceleration time series for each time step in real time according to the following relation.

$$\tau_{p,i} = 2\pi\sqrt{\frac{V_i}{A_i}}, \tag{13}$$

$$V_i = aV_{i-1} + v_i^2, \tag{14}$$

$$A_i = aA_{i-1} + \left(\frac{dv}{\mathrm{d}t}\right)_i^2. \tag{15}$$

Here, v_i is the recorded ground velocity, V_i is the smoothed ground velocity squared, A_i is the smoothed acceleration squared and a is the smoothing parameter having a value in the range of 0–1 [28]. Maximum predominant period $\tau_p^{\max}$ of a window is the value of τ_p for which the energy of the signal is maximum. Thus, the maximum dominant frequency of a selected time window can be obtained by

$$f_d = \frac{1}{\tau_p^{\max}}. \tag{16}$$

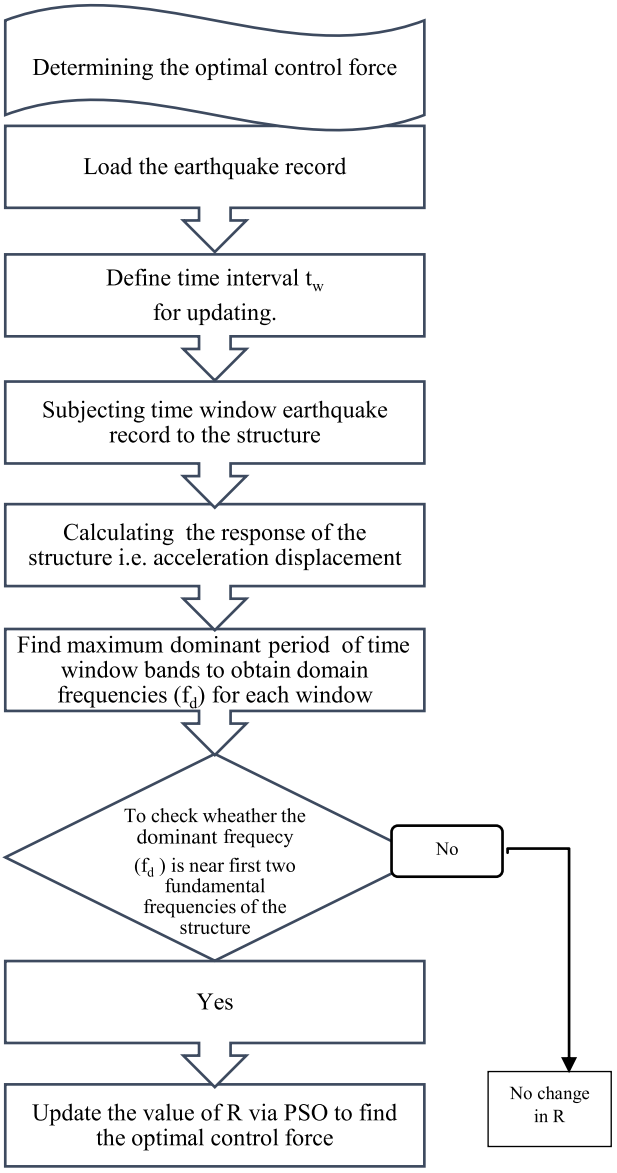

Fig. 4. Flowchart of proposed modified LQR algorithm.

This dominant frequency determines the quasi-resonance stances where the value of **R** is to be modified. Here, the PSO algorithm is used to find the optimal value of **R** that gives the optimum structural response with optimized control effort. PSO algorithm helps to find the value of **R** where the quasi-resonance occurs. The benefit of this specific local optimal solution is that it can change the estimation of matrix **R** on an odd frequency at which quasi-resonance occurs, unlike the conventional LQR which has a global value of **R** during an earthquake. The cost function to be minimized for this modified LQR problem is formulated by having state weighting matrix $\mathbf{Q_i}$ and control weighting matrix $\mathbf{R}_i$ for ith window and is given in equation (17)

$$J_i(x,u) = \int_0^{t_i} \left(x^T Q_i x(t) + f^T R_i f(t)\right) dt. \tag{17}$$

The result of this modified optimal control problem with cost function J_i leads to a control force for the ith window given in equation (18)

$$f_i = -[G_i]x. \tag{18}$$

The solution of Ricatti matrix differential equation [29] for every windowed interval gives the gain matrix $[G_i]$ and the anticipated control force required to counter the effect of quasi-resonance can be found by applying this force to the ith window. The flowchart is shown in Figure 4 for the advised algorithm that contains all steps in order.

4 Validation of the proposed approach through a numerical example

To examine the practicality of the proposed approach, a model of a three-story building configured with a single MR damper as shown in Figure 5 is considered. If the whole system is in linear region, the equations of motion are given as in equation (19)

$$M_p\ddot{x} + C_p\dot{x} + K_p x = \Lambda f - M\Gamma\ddot{x}_g. \tag{19}$$

M_p, C_p and K_p are the mass, damping and stiffness matrices of the structure respectively. $\ddot{x}_g$ is ground acceleration in one direction and x is a vector of the relative displacements, f is the control force, Γ is a column vector of ones, and the vector Λ is determined by MR damper's position in the structure. This three-story test structure is well explored at the Structural Dynamics and Control/Earthquake Engineering Laboratory at the University of Notre Dame [4,30,31]. The displacement of the MR damper is equal to the first-floor relative displacement, i.e. $x_{\mathrm{MR}} = x_1$ because damper is mechanically connected between ground and first floor.

$$M_p = \begin{bmatrix} 98.3 & 0 & 0 \\ 0 & 98.3 & 0 \\ 0 & 0 & 98.3 \end{bmatrix} \mathrm{kg}, \tag{20}$$

$$C_p = \begin{bmatrix} 175 & -50 & 0 \\ -50 & 100 & -50 \\ 0 & -50 & 50 \end{bmatrix} \mathrm{N\,s\,m^{-1}}, \tag{21}$$

$$K_p = \begin{bmatrix} 12 & -6.84 & 0 \\ -6.84 & 13.7 & -6.84 \\ 0 & -6.84 & 6.84 \end{bmatrix} \times 105\,\mathrm{Nm^{-1}}. \tag{22}$$

The structural measurements required for determination of apt control action are the absolute accelerations of all three floors and the MR damper displacement (i.e.$=[x_{a1}, x_{a2}, x_{a3}, x_{\mathrm{MR}}]$). The equation of motion can be written in the state space from equations (23)–(24) by defining

$$\dot{x} = Ax + Bf + E\ddot{x}_g, \tag{23}$$

$$y = Cx + Df + \upsilon. \tag{24}$$

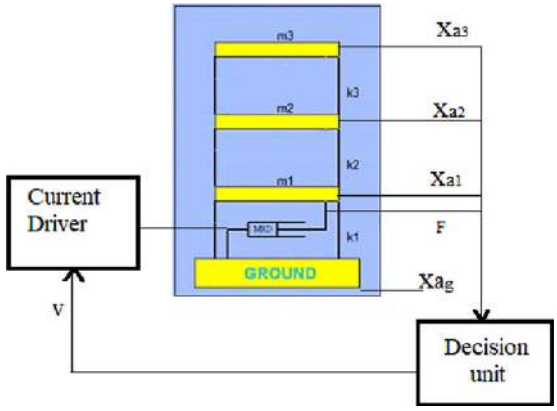

Fig. 5. A Three-story prototype structure integrated with MR damper on ground floor.

Here x is the state vector, y is the vector of measured outputs, and υ is the measurement noise vector. System matrix **A**, input matrix **B**, output matrix **C** and input-output coupling matrix **D** are given as in equations (25) and (26).

$$A = \begin{bmatrix} 0 & I \\ -{M_p}^{-1}K_p & -{M_p}^{-1}C_p \end{bmatrix} \quad B = \begin{bmatrix} 0 \\ -{M_p}^{-1}\Gamma \end{bmatrix}, \quad (25)$$

$$C = \begin{bmatrix} -{M_p}^{-1}K_p & -{M_p}^{-1}C_p \\ 1 \quad 0 \quad 0 & 0 \quad 0 \quad 0 \end{bmatrix}$$

$$D = \begin{bmatrix} -{M_p}^{-1}\Gamma \\ 0 \end{bmatrix} \quad \boldsymbol{E} = \begin{bmatrix} 0 \\ \Lambda \end{bmatrix}. \quad (26)$$

For excitation to this structure, three near-fault earthquakes time histories are considered. These earthquake ground motions are named as (i) 1940 El Centro earthquake USA (ii) 1990 Chi-Chi earthquake Taiwan (iii) 1999 Gebze Turkey earthquake. The abrupt and impulsive nature of the near-fault earthquakes makes structural control more challenging.

5 Results and discussion

In this work, the effectiveness of the suggested modified LQR controller is examined for a three DOF test structure having single MR damper on the ground floor. The cumulative energies contained in the top floor of the uncontrolled and controlled structure have also been computed and compared. It is an indicator of the shaking capability of the signal. The cumulative energy W for a signal $x(t)$ is given by the following equation (27)

$$W = \int_0^t |x(t)|^2 dt. \quad (27)$$

The state weighting matrix Q is the same as in the conventional LQR [9] for every time window. The results of first 5 s for El-Centro and Gebze and 20 s for Chi-Chi earthquake time histories respectively have been shown for better visibility. The time-histories of the response of the structure for El-Centro earthquake, Chi-Chi earthquake Gebze and earthquake are plotted in Figures 6–8.

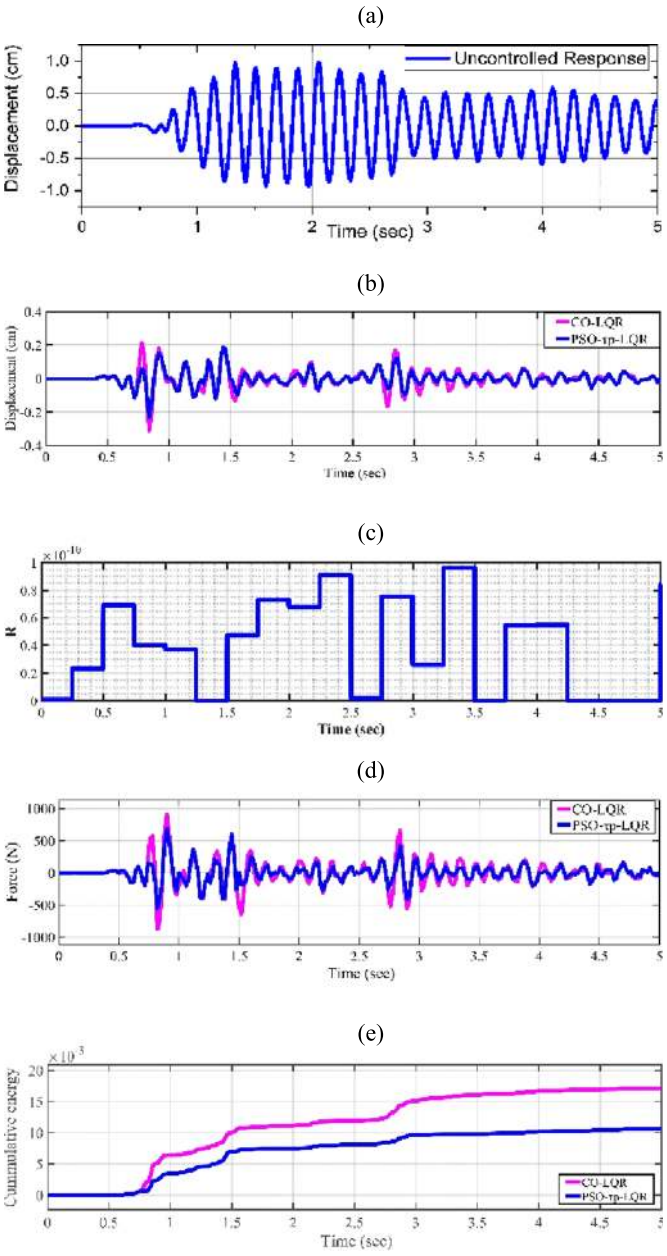

Fig. 6. Results of the top floor of the structure for the 1940 El-Centro Valley earthquake (a) displacement response of the uncontrolled structure (b) Comparison of the time history of the displacement response due to clipped optimal LQR and modified LQR (c) Variation of control weighting matrix **R** with time(d) Comparison of the time history of the force of clipped optimal LQR and modified LQR (e) Cumulative energies of the top floor of the modified controller and clipped optimal LQR controller.

First, the outcomes of numerical analysis for El-Centro valley earthquake are discussed. The relative displacement response of the uncontrolled structure is shown in Figure 6a.

The comparison of the controlled displacement time-histories of third floor for the conventional clipped optimal LQR and the proposed modified LQR algorithm is

Table 1. Peak responses of the structure due to 1940 El-Centro, 1999 Chi-Chi, and 1999 Gebze Turkey earthquake.

Control algorithm	El-Centro earthquake			Chi-Chi earthquake			Gebze earthquake		
	Uncontrolled	Clipped optimal LQR	Modified LQR	Uncontrolled	Clipped optimal LQR	Modified LQR	Uncontrolled	Clipped optimal LQR	Modified LQR
Displacement (cm)	0.55	0.09	0.07(−23)	0.14	0.03	0.02(−33)	0.0741	0.021	0.020(−5)
	0.83	0.20	0.16(−19)	0.22	0.05	0.03(−40)	0.1165	0.0342	0.030(−12)
	0.97	0.31	0.23(−24)	0.27	0.06	0.04(−34)	0.1381	0.0600	0.050(−17)
Inter story drift (i_d) (cm)	0.55	0.09	0.07(−23)	0.14	0.021	0.02(−5)	0.074	0.021	0.020(−5)
	0.29	0.10	0.09(−15)	0.08	0.02	0.01(−50)	0.042	0.017	0.010(−43)
	0.14	0.11	0.07(−33)	0.05	0.011	0.01(−9)	0.022	0.026	0.020(−22)
Acceleration (cm/s^2)	870	474	266(−44)	181	38	36(−6)	126	81	59(−28)
	1070	540	465(−14)	268	63	59(−6)	150	95	68(−28)
	1400	772	525(−32)	317	101	96(−5)	185	114	110(−4)
Force (N)	0	984	737(−25)	0	1398	1190(−15)	0	1080	1050(−3)

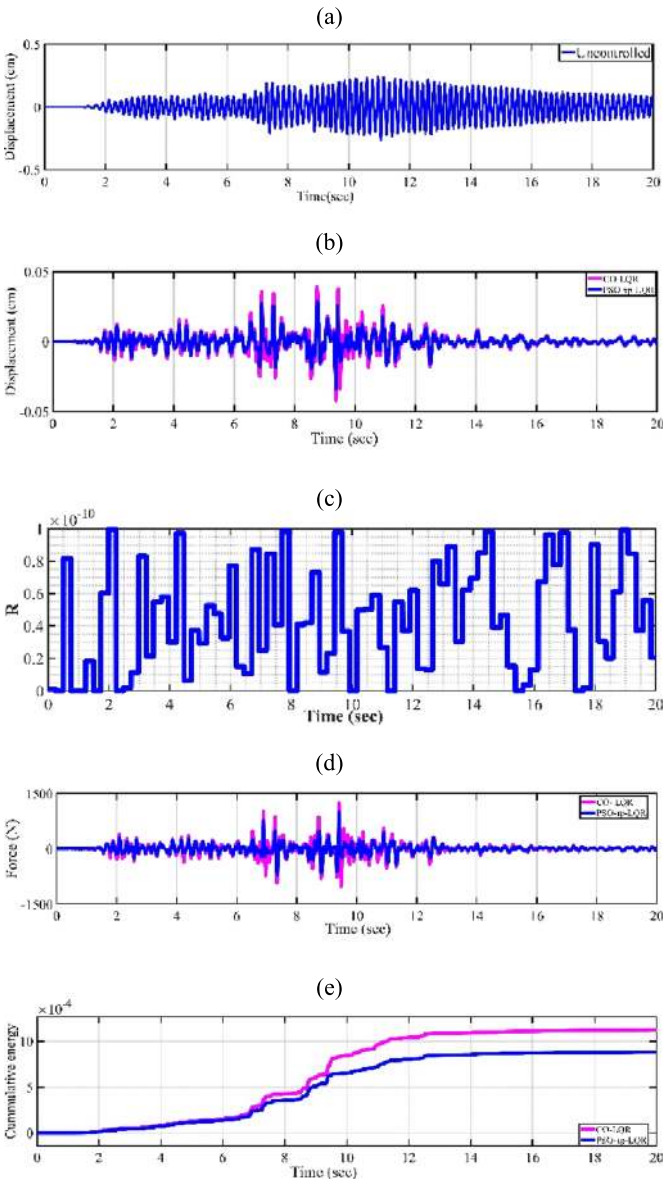

Fig. 7. Results of the top floor of the structure for the 1999 Chi-Chi earthquake (a) displacement response of the uncontrolled structure (b) Comparison of the time history of the displacement due to clipped optimal LQR and modified LQR (c) Variation of control weighting matrix **R** with time(d) Comparison of the time history of the force of clipped optimal LQR and modified LQR (e) Cumulative energies of the top floor of the modified controller and clipped optimal LQR controller.

represented in Figure 6b. This comparison clearly shows that the proposed algorithm reduces the relative displacement effectively during the earthquake.

The variation in the value of weighting matrix **R** is shown in Figure 6c. For conventional LQR controller, the value of **R** remains the same during the earthquake while for suggested approach, its value is optimized using PSO algorithm according to the quasi-resonance between the structure and the earthquake. The comparison of the time-histories of control force due to the conventional clipped optimal LQR and the proposed modified LQR algorithm is

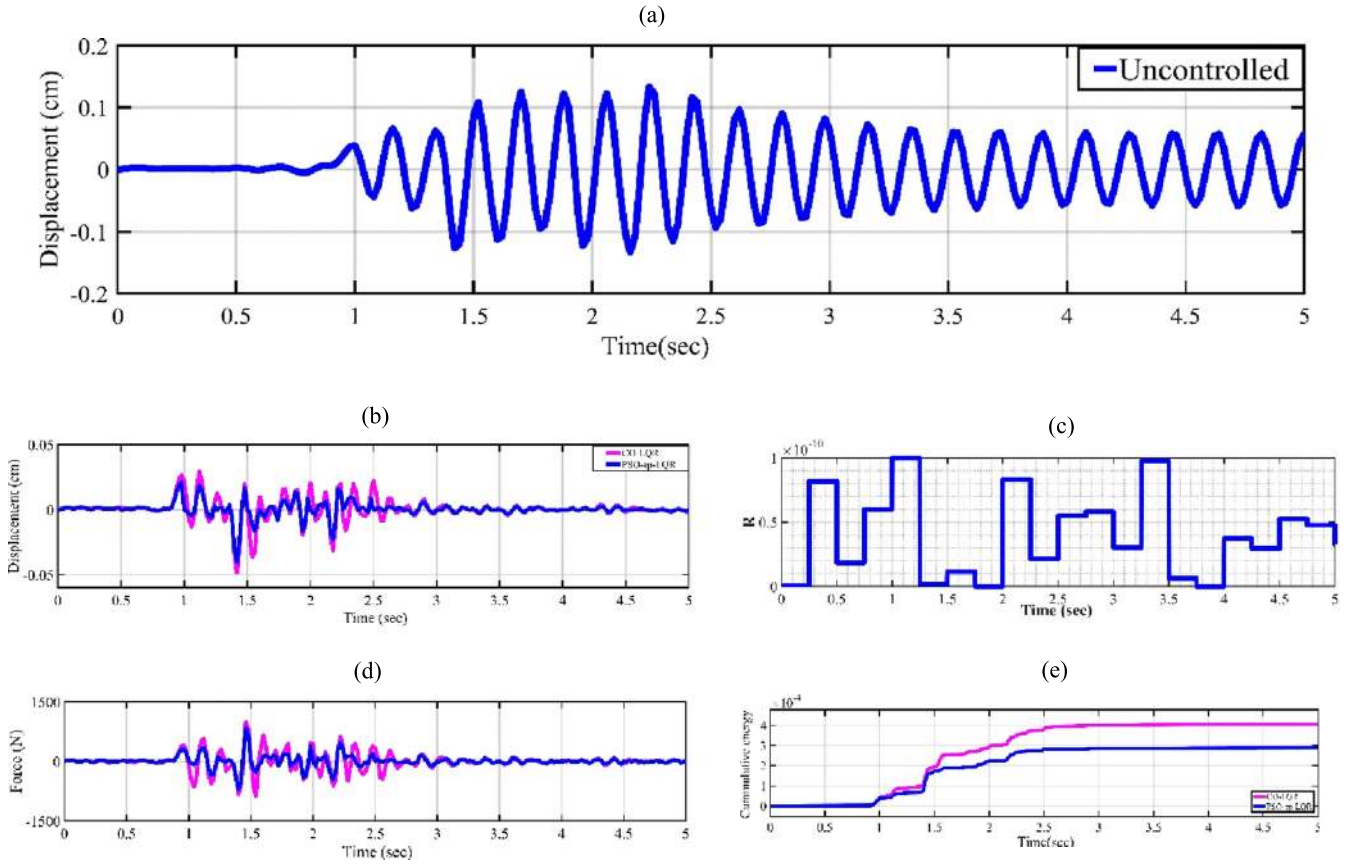

Fig. 8. Results of the top floor of the structure for the 1999 Gebze Turkey earthquake (a) displacement response of the uncontrolled structure (b) Comparison of the time history of the displacement response due to the clipped optimal LQR and modified LQR (c) Variation of control weighting matrix **R** with time (d) Comparison of the time history of the force of clipped optimal LQR and modified LQR (e) Cumulative energies of the top floor of the modified controller and conventional LQR controller.

represented in Figure 6d. This comparison demonstrates that the proposed algorithm requires lesser force to reduce the vibrations than the conventional LQR controller during the earthquake. The cumulative energies, contained in controlled and uncontrolled signal of the third or top floor is compared in Figure 6e. It shows that the shaking capacity of the controlled signal is reduced significantly. Table 1 enlists the peak values of relative displacement, inter-story drift $i_d\,(x_{i+1} - x_i)$ and the acceleration $(\ddot{x}_a)$. The values in parenthesis represent the percentage reduction in the peak values with respect to the conventional LQR.

From Table 1, it is observed that the modified LQR reduces the peak values of relative displacement of the first, second and third floor by 23%, 19%, and 24%, respectively in comparison to the conventional LQR controller. Likewise, the inter-story drifts between third-second floors and second- first floors are reduced by 33% and 15%, respectively in comparison to conventional LQR controller.

It means that the occupants of the top floor are safer and more comfortable using the modified controller. If the accelerations of the first, second and third floors are compared with the conventional LQR controller, these are reduced by 44%, 14%, and 32%. To achieve these reductions, the control force applied by the modified controller is also 25% lesser than applied by conventional LQR controller.

The same analysis is continued for Chi-Chi earthquake and Gebze earthquakes to ensure the consistency of the suggested modified controller. The outcomes of these simulations follow the pattern of the results achieved due to El-Centro Valley earthquake. It is observed from Table 1 that the proposed controller reduces the relative displacement of the first, second, and third floor by 33%, 40%, and 34% for Chi-Chi earthquake and by 5%, 12%, and 17%, respectively for Gebze earthquake in comparison to the conventional LQR controller. The inter-story drift between the third-second floor and the second-first floor is reduced by 9% and 50% for Chi-Chi earthquake whereas 22% and 43% for Gebze earthquake, respectively as seen from Table 1.

Similarly, the reduction of the accelerations of first second and third floors is respectively 6%, 6% and 5% for Chi-Chi earthquake whereas 22%, 28%, and 28%, respectively for Gebze earthquake. It is worth to note that these performance gains are achieved by using suggested approach that requires 15% lesser force than classical LQR approach for Chi-Chi earthquake whereas 3% lesser force for Gebze earthquake, respectively as seen from Table 1. The time histories are shown in Figures 7 and 8 and validate the above facts graphically.

The relative displacement responses of the uncontrolled structure are shown in Figure 7a due to Chi-Chi earthquake and in Figure 8a due to Gebze earthquake.

The comparison of the relative displacement time histories using conventional LQR and the modified LQR controller are shown in Figure 7b for Chi-Chi earthquake and in Figure 8b for Gebze earthquake, respectively. The graphs in Figures 7c, 8c show the variation of **R** with time for Chi-Chi and Gebze earthquake, respectively. The variation of **R** for each time window is according to the quasi-resonance between the domain frequency and first two fundamental frequencies of the structure. The graphs shown in Figures 7d, 8d show the control force time history due to the suggested controller and conventional LQR controller for Chi-Chi earthquake and Gebze earthquake, respectively. Similarly, the graphs shown in Figures 7e, 8e show the cumulative energy comparison of the third floor of the controlled structure using the suggested controller and conventional LQR controller for Chi-Chi earthquake and Gebze earthquake, respectively.

6 Conclusion

A modified LQR controller based on maximum predominant period approach is suggested and examined in this paper. This controller is developed by modifying the ordinary LQR controller by altering the control weighting matrix **R** over every small-time window as quasi-resonance occurred. The controller generates the optimized control force to counter larger structural response at quasi-resonance using the updated value of matrix **R** during the earthquake. The determination of the quasi-resonance instances is done in time domain itself in this paper. It is a remarkable improvement over the previous studies in which we need to move in the frequency domain to obtain the dominant frequency for each window. Therefore, the merit of the advised method is that the gain matrices are ascertained adaptively by PSO algorithm, unlike conventional LQR controller. The results exhibit that the proposed controller performs essentially superior to the conventional LQR controller. The inalienable adaptability in the design of the proposed controller to account for the quasi-resonance by the modification of the conventional LQR controller makes it a fascinating controller for the structural control.

Acknowledgements. The authors are very grateful to the Dr. Rajeev Sachdeva, (Project fellow) Mr. Govind Rathore and Mr. Dheeraj Raj (research scholars) of Department of earthquake engineering, Indian institute of Technology Roorkee for their valuable contributions to this work.
This research was financed by the Ministry of Human Resource and development of the Govt. of India (Grant No. MHR-02-23-200-429).

References

[1] B.C.B. Brown, J.T.P. Yao, Fuzzy sets and structural engineering, ASME J. Appl. Mech. 109 (1983) 1211–1225
[2] G.W. Housner et al., Structural control: past, present, and future, J. Eng. Mech. 123 (1997) 897–971
[3] G. Kumar, A. Kumar, Fourier transform and particle swarm optimization based modified LQR algorithm for mitigation of the vibrations using magnetorheological dampers, Smart Mater. Struct. 26 (2017) 115013
[4] B.F.J. Spencer, S.J. Dyke, M.K. Sain, J.D. Carlson, Phenomenological model for magnetorheological dampers, J. Eng. Mech. 123 (1997) 230–238
[5] S.K. Sharma, A. Kumar, Ride performance of a high-speed rail vehicle using controlled semi-active suspension system, Smart Mater. Struct. 26 (2017) 055026
[6] L.M. Jansen, S.J. Dyke, Semiactive control strategies for MR dampers: comparative study, J. Eng. Mech. 126 (2000) 795–803
[7] S.J. Dyke, L.M. Jansen, Implications of control-structure interaction in scaled structural control system testing, Proc. IEEE 1 (1999) 2–7
[8] S.J. Dyke, B.S. Jr, A comparison of semi-active control strategies for the MR damper, Intell. Inf. Syst. (1997) 580–584, https://doi.org/10.1109/IIS.1997.645424"\t"_blank"10.1109/IIS.1997.645424
[9] S.J. Dyke, B.F. Spencer, M.K. Sain, J.D. Carlson, Modeling and control of magnetorheological dampers for seismic response reduction, Smart Mater. Struct. 5 (1999) 565–575
[10] J. Liu, H.J. Liu, S.J. Dyke, Control-structure interaction for micro-vibration structural control, Smart Mater. Struct. 21 (2012) 105021
[11] K.M. Choi, S.W. Cho, H.J. Jung, I.W. Lee, Semi-active fuzzy control for seismic response reduction using magnetorheological dampers, Earthq. Eng. Struct. Dyn. 33 (2004) 723–736
[12] D. Giraldo, O. Yoshida, S.J. Dyke, L. Giacosa, Control-oriented system identification using ERA, Struct. Control Heal. Monit. 11 (2004) 311–326
[13] C.S. Chang, T.S. Liu, LQG controller for active vibration absorber in an optical disk drive, IEEE Trans. Magn. 43 (2007) 799–801
[14] Y. Wang, S. Dyke, Smart system design for a 3D base-isolated benchmark building, Struct. Control Heal. Monit. 15 (2008) 939–957
[15] P. Tan, A.K. Agrawal, Benchmark structural control problem for a seismically excited highway bridge-part II: phase I sample control designs, Struct. Control Heal. Monit. 16 (2009) 530–548
[16] X.M. Dong, M. Yu, C.R. Liao, W.M. Chen, Comparative research on semi-active control strategies for magneto-rheological suspension, Nonlinear Dyn. 59 (2010) 433–453
[17] S.Y. Zhang, X.M. Wang, Study of fuzzy-PID control in MATLAB for two-phase hybrid stepping motor, Appl. Mech. Mater. 341 (2013) 664–667
[18] Q.P. Ha, M.T. Nguyen, J. Li, N.M. Kwok, Smart structures with current-driven MR dampers: modeling and second-order sliding mode control, IEEE/ASME Trans. Mechatron. 18 (2013) 1702–1712
[19] W. Huang, J. Xu, D.Z.Y. Wu, J.L.K. Lu, Semi-active vibration control using a magneto-rheological (MR) damper with particle swarm optimization, Arab. J. Sci. Eng. 40 (2015) 747–762
[20] A. Shafieezadeh, K. Ryan, Y. Chen, Fractional order filter enhanced LQR for seismic protection of civil structures, J. Comput. Nonlinear Dyn. 3 (2008) 21404
[21] S. Das, I. Pan, K. Halder, S. Das, A. Gupta, LQR based improved discrete PID controller design via optimum selection of weighting matrices using fractional order integral performance index, Appl. Math. Model. 37 (2013) 4253–4268
[22] G.F. Panariello, R. Betti, R.W. Longman, Optimal structural control via training, J. Eng. Mech. 123 (1997) 1170–1179
[23] B. Basu, S. Nagarajaiah, A wavelet-based time-varying adaptive LQR algorithm for structural control, Eng. Struct. 30 (2008) 2470–2477

[24] B. Basu, S. Nagarajaiah, Multiscale wavelet-LQR controller for linear time-varying systems, J. Eng. Mech. 136 (2010) 1143–1151
[25] S. Talatahari, A. Kaveh, N.M. Rahbari, Parameter identification of Bouc-Wen model for MR fluid dampers using adaptive charged system search optimization, J. Mech. Sci. Technol. 26 (2012) 2523–2534
[26] P.C. Fourie, A.A.A. Groenwold, The particle swarm optimization algorithm in size and shape optimization, Struct. Multidiscip. Optim. 23 (2002) 259–267
[27] G.G. Amiri, A.A. Rad, S. Aghajari, N.K. Hazaveh, Generation of near-field artificial ground motions compatible with median-predicted spectra using PSO-based neural network and wavelet analysis, Comput. Civ. Infrastruct. Eng. 27 (2012) 711–730
[28] Y. Nakamura, J. Saita, UrEDAS, the earthquake warning system: today and tomorrow, Earthq. Early Warn. Syst. (2007) 249–281, DOI:10.1007/978-3-540-72241-0_13, ISBN: 978-3-540-72241-0
[29] M.G. Sakar, A. Akgül, D. Baleanu, On solutions of fractional Riccati differential equations, Adv. Differ. Equ. 2017 (2017) 39
[30] D.P. Serrano, C.V. Pasamontes, R.G. Moreno, Modelos animales de dolor neuropático, Dolor 31 (2016) 70–76
[31] S.J. Dyke, B.F. Spencer Jr, M.K. Sain, J.D. Carlson, An experimental study of MR dampers for seismic protection, Smart Mater. Struct. 7 (1998) 693–703

Cite this article as: G. Kumar, A. Kumar, R.S. Jakka, An adaptive LQR controller based on PSO and maximum predominant frequency approach for semi-active control scheme using MR Damper, Mechanics & Industry **19**, 109 (2018)